Colloidal magnetite nanoparticles – cytotoxicity study on V79 lung fibroblast cells

C.T. Mihai[*,****], E. Puscasu[**], L. Sacarescu[***], C. Nadejde[*,**], D. Gherghel[****], D. Creanga[**] and G. Vochita[****]

[*]Interdisciplinary Research Department – Field Science, 'Alexandru Ioan Cuza' University, Lascar Catargi Str. 54, Iasi, Romania
[**]Physics Department, 'Alexandru Ioan Cuza' University, Carol I Blvd. 11A, Iasi, Romania, claudia.nadejde@uaic.ro, mdor@uaic.ro
[***]Institute of Macromolecular Chemistry "P. Poni", Gr. Ghica Voda. Alley 41A, Iasi, Romania
[****]Institute of Biological Research, Lascar Catargi Str. 47, Iasi, Romania

ABSTRACT

Colloidal magnetic nanoparticles (MNPs) were yielded by chemical route for possible biomedical applications - being characterized through microstructural and magnetometric methods and then tested for cytotoxicty with focus on cell apoptosis and DNA fragmentation. Cytotoxicity assays were performed on Chinese hamster lung fibroblast V79 cells. MNPs tested concentrations were of 25-50-100-150-200 µg/ml. Flow cytometry investigation evidenced apoptosis inducing for certain MNP levels. The electrophoresis comet assay showed up to 50% DNA progressive damage for MNP concentration up to 100 µg/ml that remained almost the same when concentration increased to 200 µg/ml. The main hypothesis upon the phenomenological background underlying the obtained results is based on iron ions released following MNPs uptake in the cytoplasm that were able to trigger apoptosis by DNA damages as well as cell necrosis through toxic reactive oxygen species formation.

Keywords: colloidal magnetic nanosystems, lung fibroblast cells, DNA breaking, apoptotic cells

1 INTRODUCTION

Colloidal suspensions of magnetic nanoparticles (MNPs) are largely yielded and one of most challenging application domain consists in biomedical array of novel procedures such as targeted drug delivery, tissue local hyperthermia in cancer therapy, contrast agents in nuclear magnetic resonance imaging, cell separation, detoxification of biofluids, tissue repair, etc. [1-3]. Among various synthesis techniques, by high-temperature reactions, sol-gel reactions, decomposition of organometallic precursors, polyol methods and others [3,4], chemical co-precipitation remained a popular method since it is easily implemented, inexpensive compared to other technological approaches and could ensure good control on resulted product properties [5,6].

From the viewpoint of their biocompatibility, iron oxide nanoparticles, such as magnetite and maghemite are preferred due to remarkable reactivity allowing surface stabilization with various molecules and further biomolecule grafting and also because they are naturally excreted via the liver after treatment [7]. Since various bioeffects of nanoparticulate matter were reported in the last decades, beside beneficial applications in medical experimental procedures and biomedicine research scientists became interested also in MNP toxicity. It was constantly observed that the higher magnetic nanoparticle concentration the higher the bioeffects [8] while many different factors could also influence living body responses to MNPs. Except engineered nanoparticles impact, also potential risk of environmental contamination with nanoparticles is critical for magnetic ones; easiest way to enter the body is through respiratory system, which makes lung cell response to MNPs of specific interest for cytotoxicity assessing. Nanosized magnetite toxicity was tested on various cell lines of mammal organisms mostly of murine and human origin from either healthy or malign tissues; investigation methods of cell viability are focused on the evidencing of various cellular changes, either morphological or physiological ones, such as membrane integrity, mitochondrial dysfunction, oxidative stress, DNA injury, apoptosis induction, etc. In this paper we present colloidal MNPs, synthesized by coprecipitation technique, characterized by transmission electron microscopy (TEM), small angle X-ray scattering (SAXS), X-ray diffractometry (XRD) vibrating sample magnetometry (VSM), and tested for cytotoxicity on V79 lung cell line focusing on cell apoptosis and DNA strand breaks.

2 EXPERIMENTAL

2.1 Nanoparticle suspension: synthesis and characterization

All chemicals were analytical high purity reagents (Sigma-Aldrich, Lach-ner, Biochrom AG) used in experiments as received. Deionised water (18.2 MΩ/cm, Barnstead EasyPureII Ultrapure Water System) was used in all experimental procedures.

Nanoparticulated systems with iron oxide core and oleate shell with potential biomedical applications were synthesized by chemical route [9] at about 75 °C using

NaOH alkali as precipitation agent. Stoichiometric 2:1 ratio of ferric to ferrous salts (3.622 g $FeCl_3 \times 6\ H_2O$ and 1.332 g $FeCl_2 \times 4\ H_2O$ crystalline powders, each dissolved in 100 ml warm water) was stirred in a flat bottom flask placed on a magnetic plate with thermal heating. After the temperature reached 80 °C, 50 ml of 1.7 M hot NaOH was slowly added dropwise. Magnetic stirring was carried out continuously for another half hour with temperature kept over 80 °C. Ferrophase in the form of black brownish powder that resulted in the reaction medium was magnetically decanted and washed three times with 200 ml warm water, the last two being acidification steps (diluted HCl). Oleate ion was supplied from hydrosoluble sodium oleate, known to develop strongest interaction with iron ions, in order to ensure MNPs sterical stabilization in aqueous suspension. Ferrophase was mechanically homogenized for 15 minutes, then 30 ml aqueous solution of sodium oleate was gradually added under continuous vigorous stirring that was continued for another 60 minutes at high temperature. Finally, stable suspension of oleate coated magnetic nanoparticles was obtained.

2.2 MNP sample characterization

Hitachi High-Tech HT7700 Transmission Electron Microscope (TEM), was utilized to image and measure MNP physical diameter. Small-Angle X-Ray Scattering experiments (SAXS) were performed on a Nanostar U-Bruker system (Vantec 2000 detector, X-ray I μS microsource); the samples were sealed in a quartz capillary and measured under vacuum at constant temperature (25 °C) for 10000 s. Crystallinity features were analyzed with X-Ray Diffraction (XRD) device Shimadzu 6000, while magnetic properties were evidenced by Vibrating Sample Magnetometer (VSM, MicroMag model 2900/3900).

2.3 Cell cultures and investigation

The Chinese hamster lung fibroblast V79 cells were chosen for cytotoxicity investigation due to their relatively high plating efficiency and short generation time (12-14 hours). The cells were cultured in 75 cm^2 flask at $1.5 \times 10^4/cm^2$ density in DMEM medium (Dulbeco's Modified Eagle's Medium), supplemented with 10% heat inactivated fetal bovine serum, 100 µg/ml streptomycin and 100 IU/ml penicillin at 37 °C in a 5% CO_2 humidified incubator (Binder CB 150, Tuttlingen, Germany). At 90% confluence, cells were harvested using 0.25% (w/v) Trypsin - 0.53 mM EDTA solution and were sub-cultured into 24-well plates (TPP Techno Plastic Products AG, Trasadingen, Switzerland). 5×10^4 cells were distributed in every well and allowed to grow for 24 hours before treatment.

The MNPs were dispersed in complete culture medium with concentration range: 25 – 50 – 100 – 150 – 200 µg/ml. The experimental arrangement was based on triplicate samples for both cell viability and comet tests.

After 24 hours from incubation in the medium containing appropriate concentrations of MNPs, the cells were harvested by trypsinization and washed twice with cold PBS and centrifuged at 2000 rpm for 5 minutes. After the final wash the cell pellet was resuspended in binding buffer and stained successively with annexin V – FITC (fluorescein isothiocyante) and propidium iodide (PI) according to the manufacturer's instructions (eBioscience Annexin V-FITC Apoptosis Detection Kit). Thus, 500 µl binding buffer and 5 µl annexin V – FITC was added to the all samples that were incubated for 15 minutes in the darkness at room temperature. Thereafter, 5 µl propidium iodide aliquots were pipetted into the samples and kept for 5 minutes at 4 °C.

Bivariate analysis was performed on Beckman Coulter Cell Lab QuantaSC flowcytometer, the 488 nm blue laser was used for excitation and fluorescence was collected for FITC on FL1 (525 nm bandpass filter) and for PI on FL3 (670 nm long pass filter). All flow cyotmetric data were collected as LMD (list mode data) files and analyzed using Flowing Software (Cell Imaging Core, Turku Centre for Biotechnology, Åbo Akademi University, Finland).

The alkaline comet assay was conducted according to [10]. Briefly, approximately 1×10^4 cells were mixed with 1 ml of 1 % low melting point agarose and then were rapidly spread on precoated slides (1% normal melting point agarose). After the agarose solidified, the slides were immersed in freshly prepared lysis buffer (1.2 M NaCl, 100 mM Na_2EDTA, 0.1% sodium lauryl sarcosinate, 0.26 M NaOH, pH > 13) and lysed overnight. After that slides were removed from lysis solution and washed twice with alkaline rinsing solution (0.03 M NaOH, 2 mM Na_2EDTA, pH ~12.3). The washed slides were submerged in electrophoresis solution (0.03 M NaOH, 2 mM Na_2EDTA, pH ~12.3). The electrophoresis was conducted for 25 minutes within electric field of 0.6 V/cm. After that the slides were rinsed with distilled water, stained with 100 µl of ethidium bromide (20 µg/ml) and rinsed again with distilled water. Comet spots were visualized with Nikon Eclipse 600 (Nikon, Japan) epifluorescence microscope at 200× magnification. CometScore™ (version 1.5.2.6, TriTek) software was utilized to process comet test images by the evaluation of comet tail length, DNA % in tail and by calculating tail and Olive moment [11].

Statistical analysis. Student's "*t*" test was applied for the data resulted from at least three repetitions of each assay, with significance threshold $p < 0.01$.

3 RESULTS AND DISCUSSION

TEM images show polydispersity of round or discoid MNP systems with frequent size within 5–12 nm range (Fig. 1). Some particle agglomeration or association in apparently larger systems – up to 40 nm, could be the result of overlapping during solvent evaporation and ferropahse deposition onto the microscopy grid. Granulation analysis in liquid samples was expected to provide more insight on the microstructural features of the studied MNPs.

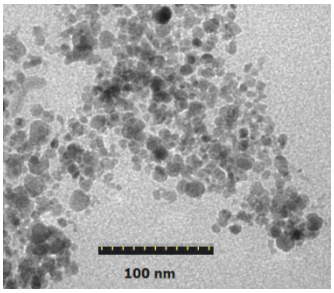

Figure 1: TEM image of MNP sample

SAXS analysis on the assumed flat nanoparticles (or short cylindric nanosystems) allowed the estimation of the averaged ferrophase size of MNPs in native suspension. For this purpose, a model free treatment of data was considered. In this approach the scattering data are plotted in a double logarithmic scale as scattering intensity (I) versus scattering vector (q). Such a graphical representation allows correlating details concerning the morphological aspects of the scatterers with the curve profile (Fig. 2). Thus, in our case, the scattering curve has the characteristic profile for discoid shape, rather flat nanosized cylinders [12].

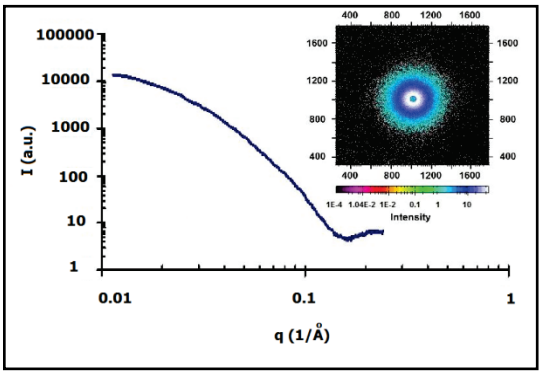

Figure 2: SAXS data analysis in log-log representation: I-intensity; q-scattering vector.

An estimation of the average dimension for these particles has resulted by calculating the radius of gyration using the Guinier plot for flat particles; the obtained averaged maximal dimension of the particles was 7.3 nm. This value is in good agreement with the above results evidenced by TEM study on the MNP sample.

Analysis of raw XRD recording confirmed spinel structured crystallites; possible partial conversion to maghemite of some magnetite nanoparticles occurred during open air manipulation.

Following magnetic characterization of colloidal ferrophase particles, the magnetization curve revealed higher grains among smaller superparamagnetic nanoparticles. This is confirmed by susceptibility curve (χ versus H) showing non-monotonous behavior in the domain of very low magnetic field. Thin hysteresis loop and moderate to low saturation magnetization (M_S = 21 emu/g in the present case) is concordant with literature reports for similar magnetization graph of maghemite sample; magnetic interactions occurring during VSM procedure could have some influence on the temporary ferrophase sample behavior, contributing to slight hysteresis.

According to flow cytometry data, cells were found in different physiological conditions related to the influence of MNPs on cellular processes. Bivariate analysis of control and MNP treated cell samples allowed the identification of alive, dead, apoptotic and preapopotic cells (Fig. 3).

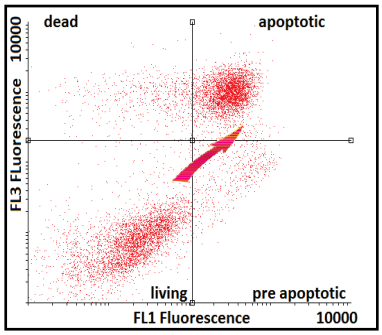

Figure 3: Flowcytometry imaging of cell distribution; fluorescence intensity (FL1 and FL3) in arbitrary units on logarithmic scale: cell sample with 50 µg/ml MNP supply

Control sample was found to contain maximal percentage of living cells (over 90%) with complementary percentage of dead cells (independent on the MNP influence) and less than one percent of apoptotic or pre-apoptotic cells. The influence of relatively low MNP concentration (50 µg/ml) remarkably increased apoptotic cell percentage (over 43%, $p < 0.01$); one could observe diminution of dead cell weight statistically balanced with living cell level (over 54%, $p < 0.05$). Dead cell frequency increasing at higher MNP doses could be determined by two complementary mechanisms: apoptosis and direct cytotoxic effect (with a smaller impact). Between 100 and 200 µg/ml no intensification of cytotoxic effect could be declared, but rather slight variations around the level was reached. We can assume that different levels of MNPs induced formation of reactive oxygen species (ROS) in different concentrations, the consequences of oxidative stress being expressed at different moments of time.

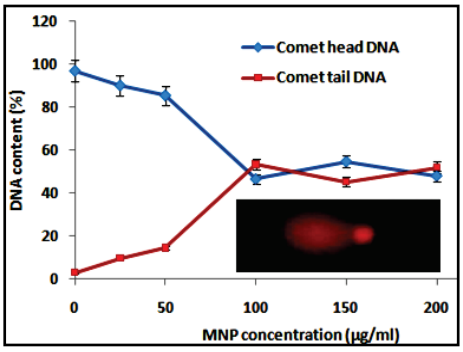

Figure 4: Quantitative estimation of DNA fragmentation

TechConnect Briefs 2015, TechConnect.org, ISBN 978-1-4987-4727-1

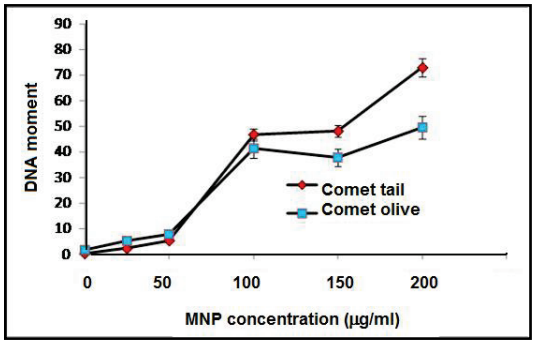

Figure 5: DNA moment versus MNP concentration

Comet assay showed that DNA clearly suffered MNP attack compared to control DNA sample where no electrophoretic nonhomogeneity on the migration slide was noticed. In Fig. 4, the influence of MNPs on cellular DNA revealed up to 50% progressive fragmentation ($p < 0.01$) for MNP concentration up to 100 µg/ml in the culture medium. Correspondingly, the amount of broken DNA strand fragments increased in the MNP supplied cells. The most important variation has been recorded between the concentrations of 50 and 100 µg/ml MNPs supplied in the cell culture medium, while for 150 and 200 µg/ml the DNA amounts varied around the level already reached for the MNP concentration of 100 µg/ml.

The graph in Fig. 5 contains information on both DNA percentage and spreading along the electric field direction. Up to 100 µg/ml MNP concentration, the evolution is very similar either in the comet tail or in its olive – with remarkable increase of almost ten folds between the MNP concentrations of 50 and 100 µg/ml. Further the damaged DNA continues to spread in the electric field, while the comet olive moment has increased with just about 10%.

MNP uptake in the cell cytoplasm, their digestion with catalytic iron ion release in the cytoplasm and further transport to the cell nucleus inducing apoptosis by oxidative stress [13], was the main hypothesis of phenomenological background for the recorded data. The lack of direct proportionality between the results of two investigation assays could be taken as proving that DNA injury evidenced by comet analysis is not the only cause of cytotoxicity revealed by cell viability assessment; this is concordant with [14] that clearly concluded on possible distinct causes of MNP cellular toxicity *in vitro* and *in vivo*: membrane leakage of lactate dehydrogenase, apoptotic bodies formation, oxidative stress induction, mithocondrial function impairment, chromosome condensation, DNA injury. Further investigation are needed to test the influence of MNP physical parameters on cell toxicity as well as to search for intimate mechanisms underlying difference in cell response when analyzed by different techniques - like flow cytometry and electrophoresis assays in the above discussed results. Nevertheless maximal attention should be paid to the concentration threshold at which iron oxide nanoparticles become toxic for actual optimization of medical procedures involving MNPs.

4 CONCLUSION

Fine granulated MNPs were prepared in stabilized colloidal suspension by means of oleate coating. Significant level of apoptotic cells was found for relatively low MNP concentration, in contrast with the case of higher MNP concentrations (where the faster mechanism of ROS triggered apoptosis occurred resulting in increased percentage of death cells at the moment of assay performing). The dependence of non-injured DNA content on the percentage of living and pre-apoptotic cells is non linear as well as the dependence of fragmented DNA content on the number of dead and apoptotic cells. The complexity of magnetic nanoparticles action on cell vital functions should be further investigated with alternative methods to get deeper insight on their cytotoxicity at different time moments and levels of cell organization.

To whom all correspondence should be addressed[1].

REFERENCES

[1] T.K. Indira, P.K. Lakshmi, Int. J. Pharm. Sci. Nanotech., 3, 1035–1042, 2010.
[2] A.B. Salunkhe, V.M. Khot, S.H. Pawar, Curr. Top. Med. Chem., 14, 1–23, 2014.
[3] D. Maity, P. Chandrasekharan, C.T. Yang, K.H. Chuang, B. Shuter, J.M. Xue, J. DingJ, S.S. Feng, Nanomed., 5,1571–1584, 2010.
[4] S. Laurent, D. Forge, M. Port, A. Roch, C. Robic, L.V. Elst, N.R. Muller, Chem. Rev., 108, 2064-2110, 2008.
[5] M.A. Willard, L.K. Kurihara, E.E. Carpenter, S. Calvin, V.G. Harris, Int. Mater. Rev., 49, 125–170, 2004.
[6] J.H. Kim, S.M. Kim, Y.I. Kim, J. Nanosci. Nanotechnol., 14, 8739–8744, 2014.
[7] A. Hajdu, E. Tombácz, E. Illés, D. Bica, L. Vékás, Progr. Colloid. Polym. Sci., 135, 29–37, 2008.
[8] V. Zavisova, M. Koneracka, J. Kovac, M. Kubovcikova, I. Antal, P. Kopcansky, M. Bednarikova, M. Muckova, J. Magn. Magn. Mater., 380, 85–89, 2015.
[9] R. Massart, IEEE Trans. Magn., 17, 1247–1248, 1981.
[10] P.L. Olive, J.P. Banáth, Nature Protocols, 1, 23–29, 2006.
[11] T.S. Kumaravel, B. Vilhar, S.P. Faux, A.N. Jha, Cell. Biol. Toxicol., 25, 53–64, 2009.
[12] O. Glatter and O. Kratky, "Small angle X-ray scattering", Academic Press, London, 1982.
[13] S. Alarifi, D. Ali, S. Alkahtani, M.S. Alhader, Trace Elem. Res., 159, 416–425, 2014.
[14] N. Singh, G.J.S. Jenkins, R. Asadi, S.H. Doak, Nano Rev., 1, 5358, 2010.

[1] C. Nadejde and D. Creanga, 'Alexandru Ioan Cuza' University, Iasi, Romania, Ph: +40(232)201064, Fax: +40(232)201150, claudia.nadejde@uaic.ro, mdor@uaic.ro.